Traffic State Estimation with the Advanced Probe Vehicles using Data Assimilation

Toru Seo, Takahiko Kusakabe, and Yasuo Asakura

***Abstract*—This paper proposes a method for estimating traffic state from data collected by the advanced probe vehicles, namely, probe vehicles with spacing measurement equipment. The probe vehicle data are assumed to include spacing information, in addition to conventional position information. The spacing information is collected as secondary products from advanced vehicle technologies, such as automated vehicles. Traffic states and a fundamental diagram are derived from the probe vehicle data. Then, a traffic state estimator based on a data assimilation technique and a traffic flow model is formulated. This procedure is intended to mitigate negative effects in traffic state estimation caused by high fluctuations in microscopic vehicular traffic. The validation results with a simulation experiment suggested that the proposed method works reasonably; for example, the proposed method was able to estimate precise traffic state compared with the previous methods. Therefore, we expect that the proposed method can estimate precise traffic states in wide area where the advanced probe vehicles are penetrated, without depending on fixed sensor infrastructures nor careful parameter calibration.**

I. Introduction

Road traffic monitoring is one of the most essential role of intelligent transport systems. In order to achieve efficient traffic management, a road administrator need to understand the traffic situation. In past half a century, various methods have been investigated and implemented to realize more effective monitoring of road traffic. Especially, recent achievements in information and communications technology have enabled us to obtain various types of information by employing a wide variety of data collection methods. Traffic situation is often defined as traffic state, which is a set of the flow, density and speed in a specific spatiotemporal point or area in a road network. Since completely continuous and long-term observation in the entire road network is practically impossible, states in unobserved area are often estimated from partially observed traffic data. This is referred to traffic state estimation (TSE) in which numerous studies have investigated, for example, [1]–[8]. Especially, probe vehicle-based TSE methods [4]–[8] have received attention due to probe vehicles' wider data collection range compared with conventional roadside detectors.

Vehicle automation technologies have begun to spread in the practical uses. Currently, these technologies are mainly utilized for microscopic-scale traffic controls, such as advanced driver assistance, autonomous driving, and vehicle-to-vehicle cooperation [9]. Meanwhile, data collected by these technologies, namely, surrounding environment of the vehicles [10], is also expected to be utilized for macroscopic traffic condition monitoring and macroscopic controls. For example, [7], [8] proposed TSE methods supposing that the spacing data from advanced vehicles are available for inputs of TSE—they referred such utilization of advanced vehicles as probes to "*probe vehicle with spacing measurement equipment* (PVSME)." In-vehicle data collection systems for similar purposes were developed by [11]–[14]. Meanwhile, the TSE methods proposed by [7], [8] do not rely on traffic flow models strongly. It implies both advantage and disadvantage: the methods can be applied for any traffic situation without information about characteristics of traffic, though the methods' estimation precision can be relatively low, especially in high resolution. One of the most significant reasons for this disadvantage is high fluctuation in microscopic vehicular traffic, such as vehicle platoons and lane-changing.

TSE methods were incorporated with traffic flow models by existing studies [1]–[6] in order to interpolate traffic states in unobserved area and/or reduce observation noises in observed area. Especially, frameworks of data assimilation (e.g., Kalman filtering-like techniques) are often utilized for TSE with traffic flow models [1]. The LWR model [15], [16] is the typical traffic flow model that represents theoretical aspect of macroscopic traffic dynamics. It represents traffic based on two important principles: the fundamental diagram (FD) and the conservation law (CL). An FD (also known as flow–density relation) determines relation among flow, density and speed. Therefore, it plays significant role in the LWR model (and many other traffic flow models), although its functional form and parameters are uncertain in actual traffic. It made existing GPS-equipped probe vehicle-based TSE methods, such as [4]–[6], applicability low; because they require careful FD's parameter calibration based on exogenous information, such as detector data (a detector-based TSE method can endogenously estimate FD's parameters [2], [3]).

The aim of this paper is to propose a PVSME-based TSE method that is robust against the high fluctuation in microscopic vehicular traffic. To mitigate the fluctuation, the proposed TSE method is incorporated with macroscopic traffic flow model with an FD and a CL (i.e., the LWR model) by using data assimilation. Since an FD is equivalent to a headway–spacing relation which is included in the PVSME data, it can be estimated endogenously. By comparing to the conventional GPS-equipped probe vehicle-based TSE methods, the proposed method can be almost self-sufficient; because it is not required to predetermine FD parameters. This makes the proposed method's applicable range wider, if the advanced vehicles have penetrated in the real world. The remainder of this paper is organized as follows. Part II describes formulation of the TSE method. Part III investigate numerical characteristics of the TSE method through a simulation experiment.

T. Seo, T. Kusakabe and Y. Asakura are with the Tokyo Institute of Technology. Email: t.seo@plan.cv.titech.ac.jp (T. Seo)

Part of this work was financially supported by the Research Fellow (DC2) program of the Japan Society for the Promotion of Science (KAKENHI Grant-in-Aid for JSPS Fellows #26010218).

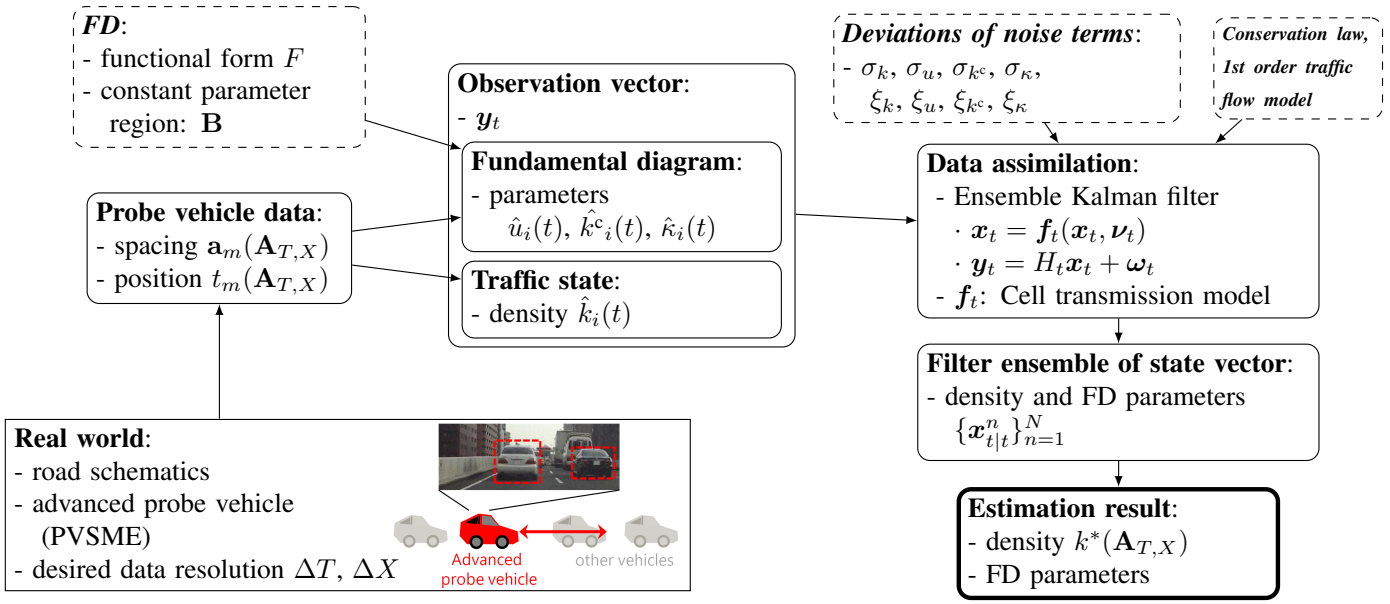

Fig. 1. Illustrated concept of the procedure of the proposed TSE method. The notation is defined at parts II-B and II-C.

II. Method

This part describes formulation of the proposed TSE method within a framework of data assimilation.

A. Concept

The following conditions are assumed for traffic that is subject of TSE in this study. The road schematics (e.g., position and length of links, link connectivity, position of nodes, number of lanes) are pre-given information for the proposed method. Probe vehicles are randomly distributed in traffic with unknown penetration rate. The probe vehicles are PVSMEs, which continuously collect data including spacing (i.e., distance between probe vehicle and its leading vehicle ahead) and position without error. Note that to measure spacing by probe vehicles, vehicle length is needed to be derived somehow.

The procedure of the proposed TSE method can be described as follows. First, time–space resolution for TSE, time–space resolution for FD's parameter estimation, and FD's functional form are set by analysts. Then, traffic states and FD parameters are respectively derived (i.e., observed) from the probe vehicle data. Finally, by using a data assimilation technique, traffic states are updated from the observed traffic states, the observed FD parameters, estimated traffic states in the previous timestep, and a traffic flow model.

Specifically, the TSE method proposed by [7] is utilized for observing traffic states. FD parameters are derived by regressing spacing and headway (spacing divided by speed) relation in the probe vehicle data. The cell transmission model [17], a numerical computation method for solving the LWR model, is applied for the traffic flow model. As a data assimilation technique, Ensemble Kalman Filter (EnKF) [18] is employed due to its capability for dealing nonlinear phenomena in traffic (the system model). Note that the observation model of the proposed TSE method can be represented by a linear system; therefore, EnKF is an appropriate way for this problem. Figure 1 summarizes the procedures of the proposed method.

B. Ensemble Kalman Filter

This part briefly describes EnKF by employing the expressions from [19].

A state–space model for EnKF can be described as follows

$$\boldsymbol{x}_t = \boldsymbol{f}_t(\boldsymbol{x}_t, \boldsymbol{\nu}_t), \tag{1}$$
$$\boldsymbol{y}_t = H_t\boldsymbol{x}_t + \boldsymbol{\omega}_t, \tag{2}$$

where eq (1) is a system equation, eq (2) is an observation equation, $\boldsymbol{x}_t$ is a state vector, $\boldsymbol{f}_t$ is a system model, $\boldsymbol{\nu}_t$ is a system noise vector, $\boldsymbol{y}_t$ is an observation vector, H_t is an observation matrix, and $\boldsymbol{\omega}_t$ is an observation noise vector, at timestep t respectively. The observation noise vector $\boldsymbol{\omega}_t$ follows normal distribution whose average is 0 and variance-covariance matrix is R_t, namely, $\boldsymbol{\omega}_t \sim \mathcal{N}(0, R_t)$.

The general procedure of EnKF can be described as follows:

Step 1 Generate an ensemble of the initial states $\{\boldsymbol{x}^n_{0|0}\}^N_{n=1}$. Let $t \leftarrow 1$.
Step 2 Prediction step:
  Step 2.1 Generate an ensemble of the system noises $\{\boldsymbol{\nu}^n_t\}^N_{n=1}$.
  Step 2.2 Calculate $\boldsymbol{x}^n_{t|t-1} = \boldsymbol{f}_t(\boldsymbol{x}^n_{t-1|t-1}, \boldsymbol{\nu}^n_t)$ for each n.
Step 3 Filtering step:
  Step 3.1 Generate an ensemble of the observation noises $\{\boldsymbol{\omega}^n_t\}^N_{n=1}$.
  Step 3.2 Obtain the filter ensemble $\{\boldsymbol{x}^n_{t|t}\}^N_{n=1}$ for each n, by calculating eq (3) based on $\boldsymbol{y}_t$, H_t, R_t, $\{\boldsymbol{x}^n_{t|t-1}\}^N_{n=1}$, $\{\boldsymbol{\omega}^n_t\}^N_{n=1}$.
Step 4 Increment the timestep, $t \leftarrow t+1$. Go back to Step 2 until $t = t_{\max}$.

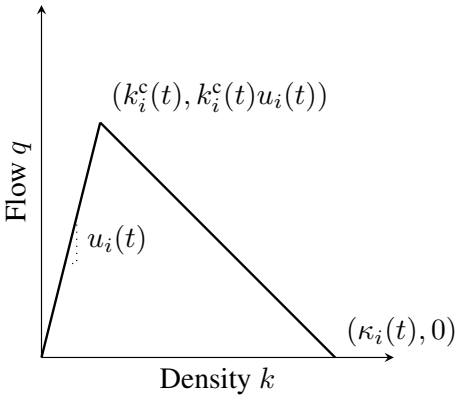

Fig. 2. Triangular FD and its parameters in cell i at time t.

The filter ensemble in Step 3.2 can be derived as follows:

$$\boldsymbol{x}_{t|t}^n = \boldsymbol{x}_{t|t-1}^n + \hat{K}_t \left(\boldsymbol{y}_t + \breve{\boldsymbol{\omega}}_t^n - H_t \boldsymbol{x}_{t|t-1}^n \right), \tag{3}$$

where,

$$\hat{K}_t = \hat{V}_{t|t-1} H_t' \left(H_t \hat{V}_{t|t-1} H_t' + R_t \right)^{-1}, \tag{4a}$$

$$\hat{V}_{t|t-1} = \frac{1}{N-1} \sum_{j=1}^{N} \breve{\boldsymbol{x}}_{t|t-1}^j (\breve{\boldsymbol{x}}_{t|t-1}^j)', \tag{4b}$$

$$\breve{\boldsymbol{x}}_{t|t-1}^n = \boldsymbol{x}_{t|t-1}^n - \frac{1}{N} \sum_{j=1}^{N} \boldsymbol{x}_{t|t-1}^j, \tag{4c}$$

$$\breve{\boldsymbol{\omega}}_t^n = \boldsymbol{\omega}_t^n - \frac{1}{N} \sum_{j=1}^{N} \boldsymbol{\omega}_t^j. \tag{4d}$$

In this study, following mean vector of the filter ensemble is defined as an "estimation result" at timestep t:

$$\bar{\boldsymbol{x}}_{t|t} = \frac{1}{N} \sum_{n=1}^{N} \boldsymbol{x}_{t|t}^n, \qquad \forall t. \tag{5}$$

C. TSE Method Formulation

In this part, the TSE method is formulated by specifying the terms and the function in eqs (1) and (2).

1) System Equation: A nonlinear system equation that represents traffic dynamics is formulated.

The state vector $\boldsymbol{x}_t$ is defined as follows:

$$\begin{aligned} \boldsymbol{x}_t = \big(& k_1(t), k_2(t), \dots, k_i(t), \dots k_M(t), \\ & u_1(t), u_2(t), \dots, u_i(t), \dots u_M(t), \\ & k_1^c(t), k_2^c(t), \dots, k_i^c(t), \dots k_M^c(t), \\ & \kappa_1(t), \kappa_2(t), \dots, \kappa_i(t), \dots \kappa_M(t) \big) \end{aligned} \tag{6}$$

where, $k_i(t)$ is a density, $u_i(t)$ is a free flow speed, $k_i^c(t)$ is a critical density, and $\kappa_i(t)$ is a jam density, of cell i at timestep t respectively. Note that $k_i(t)$ is the traffic state and $u_i(t), k_i^c(t), \kappa_i(t)$ are the FD parameters. The number of elements in vector $\boldsymbol{x}_t$ is $4M$, where M is total number of discretized spaces (cells) in the system model.

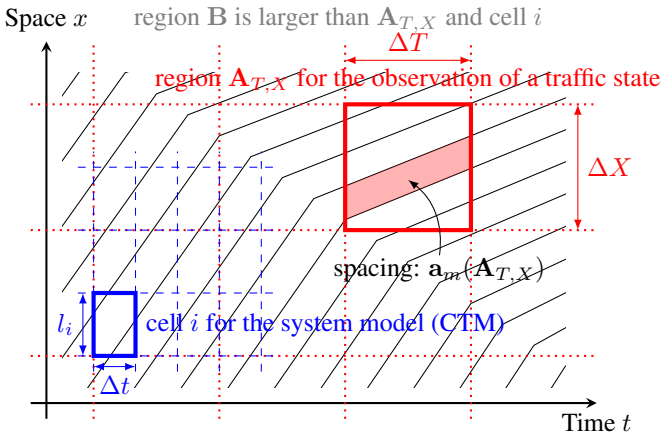

Fig. 3. Coordinates for the proposed TSE method and the probe vehicle data: solid curves represent vehicle trajectories; dotted grid represents regions for the observation; dashed gird represents cells for the system model.

The system model $\boldsymbol{f}_t$ consists of two parts: on traffic state dynamics and on FD parameters.

The first part of the system model $\boldsymbol{f}_t$ (on traffic state dynamics) is the CTM with noise term. It is described as follows:

$$Q_i^{\text{in}}(t) = \varepsilon_i^k(t) \min \left\{ \begin{array}{l} l_{i-1} k_{i-1}(t), \\ \frac{k_i^c(t)}{\kappa_i(t) k_i^c(t)} (l_i \kappa_i(t) - l_i k_i(t)) \end{array} \right\}, \tag{7a}$$

$$k_i(t+1) = k_i(t) + Q_i^{\text{in}}(t)/l_i - Q_{i+1}^{\text{in}}(t)/l_i, \tag{7b}$$

where $Q_i^{\text{in}}(t)$ is a number of vehicles that enters cell i at timestep t, l_i is the length of cell i, and $\varepsilon_i^k(t)$ is a system noise of cell i at timestep t that is expressed as $\varepsilon_i^k(t) \sim \mathcal{N}(1,\ \sigma_k^2)$ (truncated to non-negative values). Triangular FD is employed by eq (7); the relation between triangular FD and its parameters is shown in figure 2. The original CTM [17] represents traffic dynamics by solving the LWR model (partial differential equation system of continuous fluid approximated traffic) using the Godunov scheme; it can be represented as eq (7) without the noise term, $\varepsilon_i^k(t)$.

The CTM requires time and space discretization. The size of the CTM's timestep is Δt. The cell length should be equal to the timestep size multiplied by the free flow speed in the cell (i.e., $l_i = \Delta t u_i$) in order to keep consistency with the LWR model; and should be larger than the value in order to satisfy the CFL condition. The detailed discretization method is described in the next part II-C2, eq (14) and figure 3, because it has significant relation with the observation.

The other part of the system model $\boldsymbol{f}_t$ (on FD parameters) is assumed to be random walks. They can be represented as

$$u_i(t+1) \sim \mathcal{N}(u_i(t), \sigma_u^2), \tag{8a}$$

$$k_i^c(t+1) \sim \mathcal{N}(k_i^c(t), \sigma_{k^c}^2), \tag{8b}$$

$$\kappa_i(t+1) \sim \mathcal{N}(\kappa_i(t), \sigma_\kappa^2), \tag{8c}$$

where σ_u, σ_{k^c} and σ_κ are deviations for the random walks. The size of the deviations are given by the analysts.

The system noise vector $\boldsymbol{\nu}_t$ is assumed to be consists of σ_k, σ_u, σ_{k^c} and σ_κ without time, space nor flow dependency.

2) Observation Equation: A linear observation equation can be formulated based on the previous study [7].

The observation vector $\boldsymbol{y}_t$ is defined to have the same property with the state vector $\boldsymbol{x}_t$ as

$$\boldsymbol{y}_t = \left(\dots, \hat{k}_i(t), \dots, \hat{u}_i(t), \dots, \hat{k^{\mathrm{c}}}_i(t), \dots, \hat{\kappa}_i(t), \dots \right) \quad (9)$$

where the $\hat{}$ mark indicates that the variable is directly derived (i.e., observed) from the probe vehicle data. The number of elements in vector $\boldsymbol{y}_t$ is also $4M$.

From the probe vehicle data, a density in a time–space region can be derived as follows [7]:

$$\hat{k}(\mathbf{A}_{T,X}) = \frac{\sum_{m \in \mathbf{P}(\mathbf{A}_{T,X})} t_m(\mathbf{A}_{T,X})}{\sum_{m \in \mathbf{P}(\mathbf{A}_{T,X})} |\mathbf{a}_m(\mathbf{A}_{T,X})|}, \quad (10)$$

where, $\mathbf{A}_{T,X}$ is a time–space region, $\hat{k}(\mathbf{A}_{T,X})$ is an estimated generalized density in $\mathbf{A}_{T,X}$, $\mathbf{P}(\mathbf{A}_{T,X})$ is a set of all the probe vehicles in $\mathbf{A}_{T,X}$, $t_m(\mathbf{A}_{T,X})$ is a total time spent by vehicle m in $\mathbf{A}_{T,X}$, and $|\mathbf{a}_m(\mathbf{A}_{T,X})|$ is an area of a time–space region $\mathbf{a}_m(\mathbf{A}_{T,X})$, which is a time–space region between vehicle m and its leading one in $\mathbf{A}_{T,X}$. This is the observed state. The region $\mathbf{a}_m(\mathbf{A}_{T,X})$ is the key information collected by the PVSMEs. The definition of $\mathbf{A}_{T,X}$ is

$$\mathbf{A}_{T,X} = \{(x,t) \mid X \le x \le X + \Delta X,\ T \le t \le T + \Delta T\} \quad (11)$$

where ΔT and ΔX are predetermined resolutions for time and space, respectively. Equation (11) means that region $\mathbf{A}_{T,X}$ is a rectangle in time–space plane with time length ΔT and space length ΔX (c.f., figure 3).

The FD parameters are derived from regression of headway–spacing relation in the probe vehicle data. Values of $\hat{u}_i(t)$, $\hat{k^{\mathrm{c}}}_i(t)$, $\hat{\kappa}_i(t)$ are assumed to be constant in a predeterminded time–space region $\mathbf{B}$ (i.e., the observed FD parameters are constant in $\mathbf{B}$). They can be determined as

$$\hat{u}_i(t) = u(\mathbf{B}), \qquad \forall (t,i) \in \mathbf{B} \quad (12a)$$

$$\hat{k^{\mathrm{c}}}_i(t) = w(\mathbf{B})\kappa(\mathbf{B})/(u(\mathbf{B}) + w(\mathbf{B})), \qquad \forall (t,i) \in \mathbf{B} \quad (12b)$$

$$\hat{\kappa}_i(t) = \kappa(\mathbf{B}), \qquad \forall (t,i) \in \mathbf{B}, \quad (12c)$$

where $u(\mathbf{B})$, $w(\mathbf{B})$ and $\kappa(\mathbf{B})$ are the free flow speed, the wave speed and the jam density, respectively, in time–space region $\mathbf{B}$. The values of $u(\mathbf{B})$, $w(\mathbf{B})$ and $\kappa(\mathbf{B})$ are the solution of the following optimization problem:

$$\underset{u(\mathbf{B}),w(\mathbf{B}),\kappa(\mathbf{B})}{\operatorname{argmin}} \sum_{(m,\tau) \in \mathbf{P}(\mathbf{B})} D\left(h_{m,\tau}, s_{m,\tau}, u(\mathbf{B}), w(\mathbf{B}), \kappa(\mathbf{B})\right)^2,$$
$$\text{s.t. } u(\mathbf{B}) \ge 0,\ w(\mathbf{B}) \ge 0,\ \kappa(\mathbf{B}) \ge 0, \quad (13)$$

where $h_{m,\tau}$ and $s_{m,\tau}$ are stationary headway and spacing, respectively, of vehicle m at time τ, D is a function that returns the minimum distance from a point $(q,k) = (1/h_{m,\tau}, 1/s_{m,\tau})$ to a curve $q = F(k, u(\mathbf{B}), w(\mathbf{B}), \kappa(\mathbf{B}))$, and F is a function representing a triangular FD. Therefore, problem (13) finds FD parameter values that minimizes total distance between observed stationary headway–spacing points and the FD curve. Stationary means that the change rates of these variables in small time duration $\Delta\tau$ (e.g., $(h_{m,\tau} - h_{m,\tau-\Delta\tau})/h_{m,\tau}$) are small enough. This procedure is required because a theoretical FD is defined under stationary condition and an empirical FD can be clear triangular relation under stationary condition [20].

The relation between region $\mathbf{A}_{T,X}$ for the observation and cell i at timestep t in the system model are as follows. The resolution of the observation and that of the system model can be different; because that of the observation depends on the analysts purposes, while that of the system model depends on the timestep and free flow speed in the CTM. In this study, the size of region $\mathbf{A}_{T,X}$ is set to includes one or multiple cell(s) and timestep(s) completely (i.e., without extending a cell and a timestep over multiple regions for the observation) in order to make the coordinate system concise and to avoid causing numerical errors. Specifically, the value of ΔT, Δx, Δt and l_i are determined as follows:

$$l_i = \alpha \hat{u}_i(t) \Delta t, \qquad \forall (t,i) \in \mathbf{B} \quad (14a)$$

$$\Delta T = \beta \Delta t, \quad (14b)$$

$$\Delta X = \gamma l, \quad (14c)$$

where α is a coefficient larger than or equal to 1 (equal to 1 is desirable), and β and γ are natural numbers. Figure 3 shows an example with $\alpha = 1$, $\beta = 3$ and $\gamma = 2$. The analysts can select appropriate values for Δt, α, β and γ according to their interests. Following definitions are introduced in order to represent the relation between region $\mathbf{A}_{T,X}$ and cell i at timestep t:

$$\mathbf{A}_i(t) = \mathbf{A}_{T,X}, \quad \text{if } T \le t\Delta t < (t+1)\Delta t \le T + \Delta T \text{ and } X \le x_i < x_i + l \le X + \Delta X \quad (15)$$

where x_i is a space coordinate of the upstream edge of cell i. Therefore, following relation holds true:

$$\hat{k}_i(t) = \hat{k}(\mathbf{A}_i(t)) = \hat{k}(\mathbf{A}_{T,X}). \quad (16)$$

The variance of observation noise $\boldsymbol{\omega}_t$, namely, R_t, is determined as follows. The previous study [7] showed that the precision of the estimator (10) in a region $\mathbf{A}_{T,X}$ is approximately in inverse proportion to the number of the probe vehicles in $\mathbf{A}_{T,X}$, namely, $|\mathbf{P}(\mathbf{A}_{T,X})|$. Therefore, deviations of traffic state observation noises are assumed to be inversely proportional to $|\mathbf{P}(\mathbf{A}_{T,X})|$. As a result, element (a,b) of the matrix R_t is defined as

$$R_t(a,b) = \begin{cases} \frac{\xi_k^2}{|\mathbf{P}(\mathbf{A}_a(t))|}, & \text{if } a = b \text{ and } a \le M \\ \xi_u^2, & \text{if } a = b \text{ and } M < a \le 2M \\ \xi_{k^{\mathrm{c}}}^2, & \text{if } a = b \text{ and } 2M < a \le 3M \\ \xi_\kappa^2, & \text{if } a = b \text{ and } 3M < a \le 4M \\ 0, & \text{otherwise,} \end{cases} \quad (17)$$

where ξ_k is deviation for observing traffic state, and ξ_u, $\xi_{k^{\mathrm{c}}}$ and ξ_κ are deviations for observing respective FD parameters. The size of the deviations are given by the analysts.

An element (i,i) of the observation matrix H_t represents whether the cell i is observed or not. Therefore, element (a,b) of H_t is defined as

$$H_t(a,b) = \begin{cases} 1, & \text{if } a = b \text{ and } a \le M \text{ and } |\mathbf{P}(\mathbf{A}_a(t))| > 0 \\ 1, & \text{if } a = b \text{ and } a > M \\ 0, & \text{otherwise,} \end{cases} \quad (18)$$

according to the presence of probe vehicles.

D. Summary of the proposed TSE Method

As results of the filtering steps, the filter ensemble's mean vector $\bar{\boldsymbol{x}}_{t|t}$ can be obtained. The density elements (1st to M-th elements) in the mean vectors $\bar{\boldsymbol{x}}_{t|t}$ are the final output of the TSE procedure. This estimated density is declared as $k^*(\mathbf{A}_{T,X})$ with resolution of ΔT and ΔX.

The proposed TSE method estimates traffic density $k^*(\mathbf{A}_{T,X})$ from the probe vehicle data. The probe vehicle data consist of continuous position and spacing of probe vehicles, namely, $t_m(\mathbf{A}_{T,X})$ and $\mathbf{a}_m(\mathbf{A}_{T,X})$ $\forall m \in \mathbf{P}(\mathbf{A}_{T,X})$ $\forall T, X$. The framework of EnKF with the CTM is employed for the estimation procedure. The functional form of the FD is assumed to be triangular. On the other hand, the parameters of the FD are not required to be assumed; they are endogenously estimated from probe vehicle data. Note that the proposed approach possibly employs FDs with other functional forms; and use time and/or space varying FD parameters by defining appropriate $\mathbf{B}$. The parameters regarding to time–space resolution (i.e., cell and timestep size for CTM, $\mathbf{A}$ for state observation, $\mathbf{B}$ for FD parameters observation) of the estimation are given by the analysts according to their interest. The size of the noise terms are required to be given. Note that the other variables of a traffic state, namely, flow and speed, can be easily derived from the estimated density and FD.

The method assumes that probe vehicles are representing whole traffic without biases, so that the FD parameters and traffic states can be estimated without biases. However, in mixed traffic condition with traditional vehicles and automated ones, probe vehicles may have biased driving behavior and therefore the proposed TSE method will be biased.

The method treats traffic in a link—no merging/diverging sections exist in the middle of the link. Traffic in a network with multiple links can be treated by implementing a node conservation law and a merging/diverging model in the proposed approach.

For large-scale real world application, the method may be not very costly in terms of computation and data-handling. EnKF requires less computation costs compared with other techniques like the particle filter. Data required for the method are position and spacing, which are calculated by on-vehicle systems for their own purposes; therefore, not heavy data transmission and storage are required.

III. Validation

In this part, numerical characteristics of the proposed TSE method are investigated through a simulation experiment.

A. Experiment Environment

An experiment environment is prepared as follows. To generate traffic conditions investigated in a validation analysis, Aimsun [21], microscopic traffic simulator based on a car-following and lane-changing model, is employed. The parameters of the car-following model are shown in table I. The road is an almost homogeneous freeway that has a bottleneck at the end of the section. It has two lanes and 3 km length. Based on the above setting, traffic condition for 1 hour with a queue was generated.

TABLE I. Parameters of the simulation model

Parameter name	Mean	Deviation
Desired speed (km/h)	60	10.0
Max acceleration (m/s^2)	3	0.2
Normal deceleration (m/s^2)	4	0.5
Max deceleration (m/s^2)	6	0.5
Min spacing (m)	1	0.3
Vehicle length (m)	4	0.5

The probe vehicle penetration rate P was selected from 5%, 1% and 0.5%. Two types of time–space resolution for observation were selected, namely, $(\Delta T, \Delta X) \in \{$(1 min, 300 m), (10 min, 1000 m)$\}$. The observation error is expected to be smaller as the observation resolution increased as shown in previous study [7]. In order to simplify the discussion, region $\mathbf{B}$ is set to be the entire time–space region—the FD parameters are assumed to be constant throughout the simulation.

A timestep width in the system model, Δt, was set to 0.111 min. The other variables on the resolution of the system model, namely, α, β, and γ, were set to certain values such that the cell length l_i is identical to 100 m; their exact values vary in estimation iterations, depending on observed free flow speed u and given observation resolution ΔT and ΔX. With these setting, the value of α is almost always slightly larger than 1; therefore, the CFL condition is expected to be satisfied. Above mentioned parameters are set to satisfy the conditions mentioned in part II-C2, eq (14).

The size of the noise terms were set ad hoc as follows: $\sigma_k = 0.1$, $\sigma_u = 0.5$ (m/s), $\sigma_{k^c} = 0.002$ (veh/m), $\sigma_\kappa = 0.01$ (veh/m), $\xi_k = 0.01$ (veh/m), $\xi_u = 5.0$ (m/s), $\xi_{k^c} = 0.1$ (veh/m) and $\xi_\kappa = 0.2$ (veh/m). The reason for such larger size of the observation noises was that general traffic does not always follow the triangular FD, especially at a microscopic scale. Criteria for stationary headway–spacing determination is set as less than 10% change rate during 5 s ($= \Delta\tau$). In general, if this criteria is strict, precision of FD observation will be increased. However, if the criteria is too strict compared with the total amount of data, amount of data that passes the criteria becomes few so that the precision can be low. The number of ensembles N was set to 200. In general, larger N value makes accuracy of EnKF's Monte Carlo simulation better at the cost of computation.

B. Results

Figure 4 shows traffic density as time–space diagrams, whose horizontal axes represent time, vertical axes represent space, and color represents density. In figure 4, (a) represents the ground truth value k, (b) represents observed value $\hat{k}$ with $(P, \Delta T, \Delta X) = (5\%, 1 \text{ min}, 300 \text{ m})$, and (c) represents estimated value k^* with the identical resolution. According to figure 4, the noises in the observation were reduced in the filtering result, especially at free flow areas, such as traffic before 10 min. On the other hand, difference between observed and estimated states in a congested area was not so remarkable—both were close to the ground truth states.

Figure 5 shows observed FD by probe vehicles (red line), disaggregated headway–spacing relation of vehicles (gray dots) and aggregated flow–density relation in time–space regions (blue crosses), with $(P, \Delta T, \Delta X) = (5\%, 1 \text{ min}, 300 \text{ m})$. The observed FD's parameter values were $\hat{u} = 55.4$ (km/h), $\hat{k^c} =$

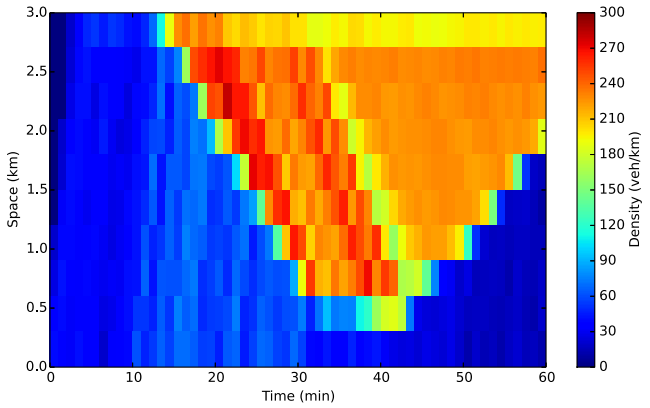

(a)

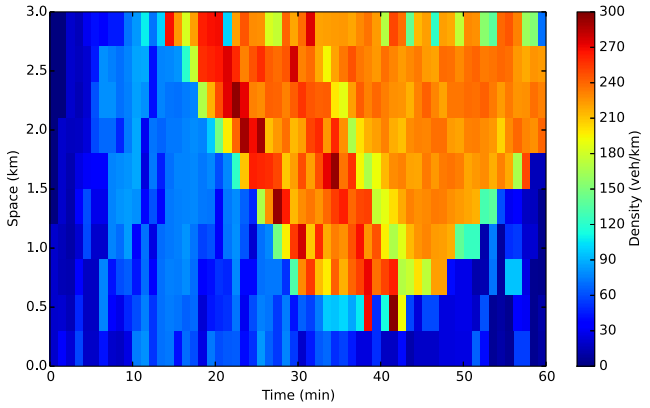

(b)

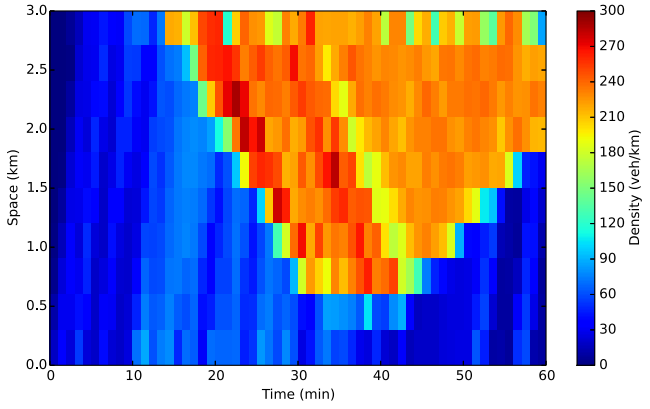

(c)

Fig. 4. Typical estimation results visualized as time–space diagrams: (a) ground truth traffic state k, (b) observed traffic state $\hat{k}$, (c) estimated traffic state k^*, RMSE(k^*)=21.7 (veh/km), and MAPE(k^*)=20.1%.

73.7 (veh/km) and $\hat{\kappa} = 388.5$ (veh/km). The disaggregated relation is widely scattered due to the high fluctuation and heterogeneity in microscopic vehicle behaviors. On the other hand, observed FD is closed to the aggregated relation which is clearly bivariate.

Table II summarizes the estimation performance. The root mean square error (RMSE) and mean absolute percentage error (MAPE) were employed as precision indices on estimated density. Their definitions were as follows: $\mathrm{RMSE}(k^*) = \sqrt{1/S \sum_{\forall(T,X)} (k(\mathbf{A}_{T,X}) - k^*(\mathbf{A}_{T,X}))^2}$, $\mathrm{MAPE}(k^*) = 1/S \sum_{\forall(T,X)} |k(\mathbf{A}_{T,X}) - k^*(\mathbf{A}_{T,X})|/k(\mathbf{A}_{T,X})$, where S is total size of the results (i.e., combination of (T, X)). The simulation were performed for 50 times in order to get the average performance. In addition, the percentage of improvement (PoI) was employed for evaluate the effect of the data assimilation. It was defined as $\mathrm{PoI}(p) = (p(\hat{k}) - p(k^*))/p(\hat{k})$, where p is a precision index, namely RMSE or MAPE. The value of PoI represents improvement of estimated density k^* compared to observed density $\hat{k}$; if the value is positive, the data assimilation worked positively for precision. According to table II, distinguishable trends can be found for precision. The precision is increased as probe vehicle penetration rate increases and time–space resolution lowers. In addition, according to PoI value, the data assimilation almost always reduced estimation error, especially on MAPE.

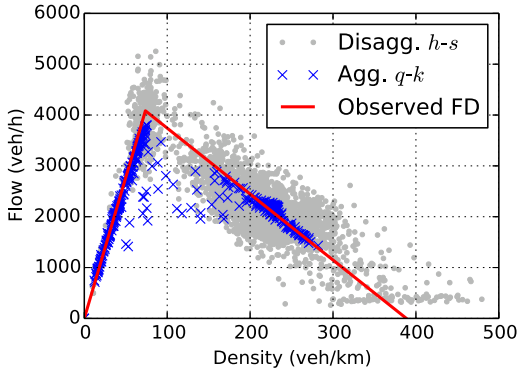

Fig. 5. Observed FD, disaggregated headway–spacing relation and aggregated flow–density relation.

C. Discussion

The results showed that the estimation precision improved due to the data assimilation in the most cases. According to figure 5, FD parameters were precisely observed by PVSMEs; therefore, the prediction steps by the traffic flow model are expected to work well. Then, according to figure 4 and table II, improvements of the estimation precision due to the filtering steps were confirmed. Especially, they were remarkable at low density regime; for example, free flow area shown in figure 4 and PoI(MAPE) in table II. This is a preferable feature for a TSE method with the PVSMEs; because the precision of the previous study's method [7] was relatively low at low density traffic. Contrary, the precision in high density (congested) regime was not improved significantly. This may be due to that the vehicular fluctuation are low in congested regime, since vehicle movements are restricted by the jam. These implied that estimation errors caused by high fluctuations in microscopic vehicular traffic were reduced as intended.

IV. Conclusions

This study proposed TSE method whose inputs are position and spacing data collected by PVSMEs (i.e., the advanced probe vehicles), which are possible secondary utilization of automated vehicles. The proposed method estimates traffic states and FD parameters jointly and endogenously from probe

TABLE II. SUMMARY ON THE ESTIMATION PERFORMANCE

Scenario parameters			Precision indices		Percentage of improvement	
P	ΔT (min)	ΔX (m)	RMSE (veh/km)	MAPE	PoI(RMSE)	PoI(MAPE)
0.5%	1	300	65.0	68.5%	8.4%	16.2%
0.5%	10	1000	31.0	12.7%	–4.3%	13.5%
1.0%	1	300	49.7	58.7%	12.6%	19.0%
1.0%	10	1000	11.6	7.5%	15.1%	21.2%
5.0%	1	300	20.3	23.0%	20.0%	29.6%
5.0%	10	1000	7.4	3.8%	5.8%	15.3%

vehicle data. In order to reduce noises, traffic states are updated using a traffic flow model-based data assimilation. As a consequence, the proposed method can be applied in anytime and anywhere regardless traffic conditions, compared with existing GPS-based TSE methods.

The results of the simulation experiment showed that the data assimilation successfully mitigated the noises in the estimation result caused by fluctuation in the microscopic vehicle behavior. Therefore, the estimation precision in higher resolution and lower probe vehicle penetration rate was increased. It means that the proposed method is robust against microscopic fluctuations, compared with the previous PVSMEs studies [7], [8], This might help precise traffic control measures.

Following future works are considerable to improve the proposed TSE approach. The first is to expand the proposed TSE approach for road network, as mentioned in part II-D. It is valuable for probe vehicle-based traffic monitoring; because it can interpolate traffic state in unobserved links where probe vehicles have not traveled, by using information from adjacent links. The second is development of methods that can correct the bias caused by probe vehicles' behavioral biases, as mentioned in part II-D, too. Possibly useful information to tackle this problem is the PVSME data themselves, by which vehicle behavior of other vehicles and probe vehicles can be estimated. The third is elimination of remained exogenous factors from the TSE method. Deviations of noise terms and a functional of an FD form are given exogenously in this study. It also includes endogenous identification method for time–space regions with constant FD. If they are determined endogenously from probe vehicle data, the applicability of the TSE method will be significantly increased. Alternatively, sensitivity analyses on the factors are required. The forth is to employ traffic flow models based on Lagrangian coordinates as a system model of the proposed TSE approach. Lagrangian traffic flow models can utilize information of trajectories of probe vehicles [5], [6], [8] so that estimation performance can be increased. The last is validation based on the real world dataset [7].

REFERENCES

[1] Y. Wang and M. Papageorgiou, "Real-time freeway traffic state estimation based on extended Kalman filter: a general approach," *Transportation Research Part B: Methodological*, vol. 39, no. 2, pp. 141–167, 2005.

[2] A. Hegyi, D. Girimonte, R. Babuska, and B. De Schutter, "A comparison of filter configurations for freeway traffic state estimation," in *Intelligent Transportation Systems Conference, IEEE*, 2006, pp. 1029–1034.

[3] Y. Wang, M. Papageorgiou, A. Messmer, P. Coppola, A. Tzimitsi, and A. Nuzzolo, "An adaptive freeway traffic state estimator," *Automatica*, vol. 45, no. 1, pp. 10–24, 2009.

[4] C. Nanthawichit, T. Nakatsuji, and H. Suzuki, "Application of probe-vehicle data for real-time traffic-state estimation and short-term travel-time prediction on a freeway," *Transportation Research Record: Journal of the Transportation Research Board*, vol. 1855, no. 1, pp. 49–59, 2003.

[5] Y. Yuan, J. W. C. van Lint, R. E. Wilson, F. van Wageningen-Kessels, and S. P. Hoogendoorn, "Real-time Lagrangian traffic state estimator for freeways," *Intelligent Transportation Systems, IEEE Transactions on*, vol. 13, no. 1, pp. 59–70, 2012.

[6] K. Wada, T. Ohata, K. Kobayashi, and M. Kuwahara, "Traffic measurements on signalized arterials from vehicle trajectories," *Interdisciplinary Information Sciences*, vol. 21, no. 1, pp. 77–85, 2015.

[7] T. Seo, T. Kusakabe, and Y. Asakura, "Estimation of flow and density using probe vehicles with spacing measurement equipment," *Transportation Research Part C: Emerging Technologies*, vol. 53, pp. 134–150, 2015.

[8] T. Seo and T. Kusakabe, "Probe vehicle-based traffic state estimation method with spacing information and conservation law," *Transportation Research Part C: Emerging Technologies*, 2015, in press, doi:10.1016/j.trc.2015.05.019.

[9] C. Diakaki, M. Papageorgiou, I. Papamichail, and I. Nikolos, "Overview and analysis of vehicle automation and communication systems from a motorway traffic management perspective," *Transportation Research Part A: Policy and Practice*, vol. 75, pp. 147–165, 2015.

[10] S. Sivaraman and M. M. Trivedi, "Looking at vehicles on the road: A survey of vision-based vehicle detection, tracking, and behavior analysis," *Intelligent Transportation Systems, IEEE Transactions on*, vol. 14, no. 4, pp. 1773–1795, 2013.

[11] S. Messelodi, C. M. Modena, M. Zanin, F. G. D. Natale, F. Granelli, E. Betterle, and A. Guarise, "Intelligent extended floating car data collection," *Expert Systems with Applications*, vol. 36, no. 3, Part 1, pp. 4213–4227, 2009.

[12] J. J. V. Diaz, D. F. Llorca, A. B. R. Gonzalez, R. Q. Minguez, A. L. Llamazares, and M. A. Sotelo, "Extended floating car data system: Experimental results and application for a hybrid route level of service," *Intelligent Transportation Systems, IEEE Transactions on*, vol. 13, no. 1, pp. 25–35, 2012.

[13] K. Yokoi, Y. Suzuki, T. Sato, T. Abe, H. Toda, and N. Ozaki, "A camera-based probe car system for traffic condition estimation," in *Proceedings of 20th ITS World Congress*, 2013.

[14] B. Coifman and H. Hall, "An overview of the on-going OSU instrumented probe vehicle research," The Ohio State University, Tech. Rep., 2014.

[15] M. J. Lighthill and G. B. Whitham, "On kinematic waves. II. a theory of traffic flow on long crowded roads," *Proceedings of the Royal Society of London. Series A. Mathematical and Physical Sciences*, vol. 229, no. 1178, pp. 317–345, 1955.

[16] P. I. Richards, "Shock waves on the highway," *Operations Research*, vol. 4, no. 1, pp. 42–51, 1956.

[17] C. F. Daganzo, "The cell transmission model: A dynamic representation of highway traffic consistent with the hydrodynamic theory," *Transportation Research Part B: Methodological*, vol. 28, no. 4, pp. 269–287, 1994.

[18] G. Evensen, "Sequential data assimilation with a nonlinear quasi-geostrophic model using Monte Carlo methods to forecast error statistics," *Journal of Geophysical Research: Oceans*, vol. 99, no. C5, pp. 10 143–10 162, 1994.

[19] T. Higuchi, Ed., *Introduction to Data Assimilation*. Asakura Publishing, 2011, (in Japanese).

[20] M. J. Cassidy, "Bivariate relations in nearly stationary highway traffic," *Transportation Research Part B: Methodological*, vol. 32, no. 1, pp. 49–59, 1998.

[21] TSS-Transport Simulation Systems, "Aimsun," www.aimsun.com.